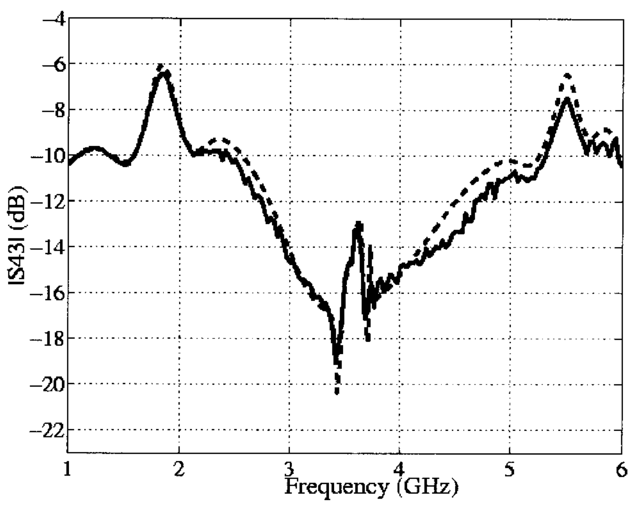

(a)

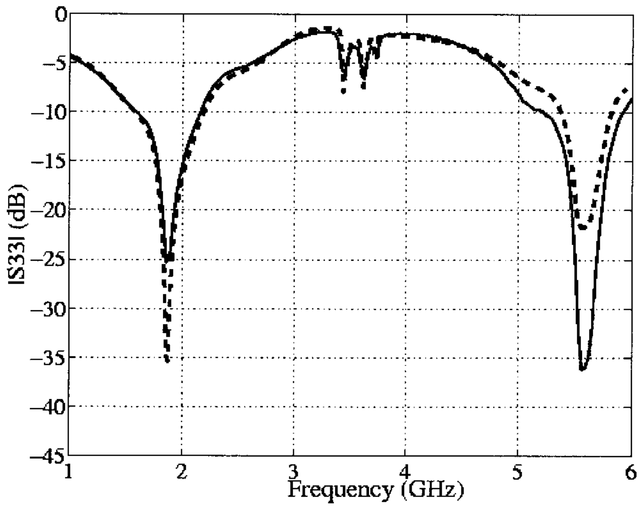

(b)

Figure 9 Comparison between simulated and experimental results: (a) transmission coefficient $|S_{43}|$; (b) reflection coefficient $|S_{33}|$. Simulation (dashed line) and measurements (solid line)

middle of the forbidden band (the narrow peaks) is caused by the phase parameter $\Delta\varphi$ of the unit cell, whereas the anisotropy parameter ($\delta/\Lambda \approx 0.067$) is responsible for their position.

The simulation results are therefore in excellent agreement with the measurements. Above 4 GHz, slight discrepancies are well explained by the imperfections from the connectors and the matched terminations.

5. CONCLUSION

We have investigated, both theoretically and experimentally, a periodic lattice made of $N \times N$ four-port networks interconnected by transmission lines, looked upon as discrete 2D photonic bandgaps of finite size. Our method is completely analytical and based upon a restricted set of so-called "canonical" parameters. The S parameters of the entire network, exhibiting typical forbidden bands, are related to the properties of the unit cell. The measurements obtained on a microwave prototype are in excellent agreement with the simulations.

Due to the simplicity of the unit cell (reciprocal, passive, and lossless), the structure studied herein should be considered as a mere prototype; the same method can be extended to more sophisticated networks. In this study, we were interested in the intrinsic response of the discrete crystal only, with all external ports matching. However, the same approach can be applied to any arbitrary boundary condition. Moreover, such a high degree of symmetry is not mandatory; the powerful approach of linear algebra would still hold in the case of symmetry breaking, as would be the case for artificial "doping" (by "defect" insertion or local network substitution). Taking the losses into account would only add one degree of freedom; besides, other classes of 2D symmetry could also be considered.

The analytical approach is not only a simple way to describe a discrete crystal, but is also a fast tool to synthesize spectral functions such as filtering, addressing, or switching. We are currently working on these kinds of potential applications.

REFERENCES

1. E. Yablonovitch, Inhibited spontaneous emission in solid-state physics and electronics, Phys Rev Lett 58 (1987), 2059.
2. S. Fan and J.D. Joannopoulos, Photonic crystals: Towards large-scale integration of optical and optoelectronic circuits, Optics Photonics News (2000), 28–33.
3. M. Thèvenot, C. Cheype, A. Reineix, and B. Jecko, Directive photonic-bandgap antennas, IEEE Trans Microwave Theory Techn 47 (1999), 2115–2121.
4. F.-R. Yang, Y. Qian, R. Coccioli, and T. Itoh, Analysis and application of photonic band-gap (PBG) structures for microwave circuits, Electromagn 19 (1999), 241–254.
5. L. Le Floc'h, V. Quintard, J.-F. Favennec, and Y. Boucher, Paramètres de répartition et bandes interdites d'un cristal photonique bidimensionnel discrétisé, J Physique IV (2002), 283–284 (in French).
6. K.C. Gupta, R. Garg, and R. Chadha, Computer-aided design of microwave circuits, Artech House, Boston, 1981, pp 197–199.

BACKWARD WAVES AND NEGATIVE REFRACTION IN UNIAXIAL DIELECTRICS WITH NEGATIVE DIELECTRIC PERMITTIVITY ALONG THE ANISOTROPY AXIS

P. A. Belov[1,2]
[1] Radio Laboratory
Helsinki University of Technology
P.O. Box 3000
FIN-02015 HUT, Finland
[2] Physics Department
St. Petersburg Institute of Fine Mechanics and Optics
Sablinskaya 14, 197101, St. Petersburg, Russia

Received 11 November 2002

ABSTRACT: *Veselago medium (also called double negative material, backward medium, left-handed medium) is a medium with both negative isotropic dielectric permittivity and permeability. It has the effect of backward waves with negative (anomalous) refraction, in contrast to the usual forward waves with normal refraction in normal isotropic dielectrics and/or magnetics. In this paper, examples of the existence of backward waves (with respect to the interface) without negative refraction, and negative refraction without backward waves in uniaxial dielectrics with negative permittivity along the anisotropy axis, are presented. Considering these examples increases the possibility of designing backward wave materials and negative*

refraction materials without using magnetic media. © 2003 Wiley Periodicals, Inc. Microwave Opt Technol Lett 37: 259–263, 2003; Published online in Wiley InterScience (www.interscience.wiley.com). DOI 10.1002/mop.10887

Key words: *backward wave; negative refraction; uniaxial dielectric*

1. INTRODUCTION

In the 1960s Veselago theoretically proposed a new class of media with extraordinary properties [1]: a material with both negative dielectric permittivity ε and magnetic permeability μ. Such a type of material is called Veselago medium. In the literature Veselago medium is also called backward medium [2, 3], left-handed medium [4–7], or double negative medium [8]. Recently, Veselago medium has attracted a lot of attention due to very interesting potential applications. The possibility of perfect lens construction was predicted by Pendry in [9]. The perfect lens design uses the property of anomalous (negative) refraction of a Veselago medium interface. The subwavelength cavity resonator design was invented by Engheta in [10] and is based on the backward wave property of Veselago medium.

There is a very important question for applications regarding possibilities of designing backward wave and/or negative refraction materials without using magnetic media. It is possible to use different kinds of photonic (electromagnetic) crystals in various regimes for this purpose [11–15]. In such media, the effects appear near spatial resonances (stopbands) of the structure, then the characteristic period of the crystal becomes comparable with the wavelength. Thus, photonic crystal can be used in the design of superlenses [14, 15], but it is impossible to use them for subwavelength cavity resonator design due to the small thickness of the media layer in comparison with the necessary wavelength.

Very interesting focusing effects (near-perfect lenses and near-field imaging) were found for slabs of negative dielectric constant isotropic materials [16–18]. It is important to consider properties of anisotropic dielectrics in order to check for backward wave and/or negative refraction effects.

In [2] the properties of uniaxial magneto-dielectrics with negative parameters were discussed in detail. It was shown that negative (anomalous) refraction for one polarization can be achieved in a uniaxial magneto-dielectric, even if only one of the four material parameters are negative. In this paper two interesting refraction effects, using uniaxial dielectrics with negative material parameters, are considered and discussed in detail. Examples of positive refraction of the wave, which is backward with respect to the interface and negative refraction of the forward wave, are possible.

2. DEFINITIONS

Trying to clarify the question about possibility of existence backward wave materials without negative refraction and/or negative refraction materials without backward waves, one needs exact definitions in order to study desired effects. In this paper the following terminology is used (for classification of homogeneous plane waves in lossless media).

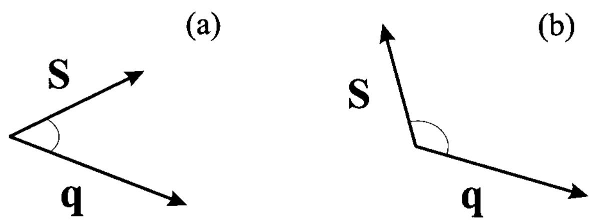

Figure 1 (a) Forward wave $\mathbf{S} \cdot \mathbf{q} \geq 0$; (b) backward wave $\mathbf{S} \cdot \mathbf{q} \leq 0$

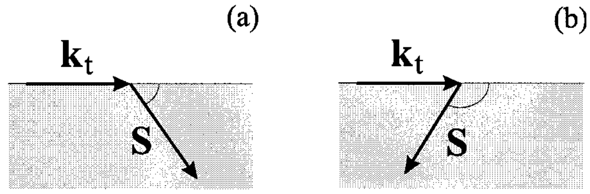

Figure 2 (a) Positive refraction $\mathbf{S} \cdot \mathbf{k}_t \geq 0$; (b) negative refraction $\mathbf{S} \cdot \mathbf{k}_t \leq 0$

(i) For the direction of wave vector $\mathbf{q}$ in the medium with respect to the energy flow (time-averaged Poynting vector $\mathbf{S}$): forward wave is a wave which has an acute angle between the wave vector $\mathbf{q}$ and the Poynting vector $\mathbf{S}$ ($\mathbf{S} \cdot \mathbf{q} \geq 0$); backward wave is a wave which has an obtuse angle between the wave vector $\mathbf{q}$ and the Poynting vector $\mathbf{S}$ ($\mathbf{S} \cdot \mathbf{q} \leq 0$).

(ii) For the direction of the energy flow (Poynting vector $\mathbf{S}$) with respect to the tangentional component of the wave vector of the incident wave $\mathbf{k}_t$ (after refraction of a plane wave coming from an isotropic dielectric): positive refraction is the phenomenon when the Poynting vector $\mathbf{S}$ of the refracted wave and tangentional component of the wave vector of incident wave $\mathbf{k}_t$ make an acute angle ($\mathbf{S} \cdot \mathbf{k}_t \geq 0$); negative refraction is the phenomenon when the Poynting vector $\mathbf{S}$ of the refracted wave and tangentional component of the wave vector of incident wave $\mathbf{k}_t$ make an obtuse angle ($\mathbf{S} \cdot \mathbf{k}_t \leq 0$).

(iii) For the direction of the wave vector $\mathbf{q}$ of the transmitted wave with respect to the interface (after refraction of a plane incident wave coming from an isotropic dielectric): forward wave with respect to the interface is a refracted wave which has an acute angle between the wave vector $\mathbf{q}$ of refracted wave and an inner interface normal $\mathbf{n}$ ($\mathbf{n} \cdot \mathbf{q} \geq 0$); backward wave with respect to the interface is a refracted wave which has an obtuse angle between the wave vector $\mathbf{q}$ of refracted wave and an inner interface normal $\mathbf{n}$ ($\mathbf{n} \cdot \mathbf{q} \leq 0$).

The property of the wave to be forward or backward is determined only by the media properties, without taking refraction problems into consideration. At the same time, the phenomena of positive/negative refraction and forward/backward waves, with respect to the interface, are determined not only by the media properties, but also by the refraction problems. The orientation of the interface with respect to the inner geometry of the media plays an important role here.

Pendry in [9] has used the negative refraction effect for focusing, and backward wave effect to have all incoming rays in phase, but the last demand can be achieved using forward waves also [14, 15]. Engheta in [10] has used the property of a wave to be backward with respect to the interface.

3. GENERAL THEORY

Let us consider the properties of non-magnetic medium with the dielectric permittivity diadic $\bar{\bar{\varepsilon}}$ in the form:

$$\bar{\bar{\varepsilon}} = \varepsilon\_\mathbf{xx} + \varepsilon(\mathbf{yy} + \mathbf{zz}), \tag{1}$$

with $\varepsilon\_ < 0$, $\varepsilon > 0$. Such material will be called negative uniaxial dielectric.

Propagation of a plane electromagnetic wave with real wave vector **q**, electric field **E**, and magnetic field **H** in such media can be described using a Maxwell's equation in the following form:

$$\begin{cases} -j(\mathbf{q} \times \mathbf{H}) = j\omega\bar{\bar{\varepsilon}} \cdot \mathbf{E} \\ -j(\mathbf{q} \times \mathbf{E}) = -j\omega\mu_0\mathbf{H} \end{cases} \quad (2)$$

By substituting Eq. (2) into Eq. (1), we obtain following equation:

$$([\mathbf{q} \times [\mathbf{q} \times \bar{\bar{I}}]] + \mu_0\omega^2\bar{\bar{\varepsilon}}) \cdot \mathbf{E} = 0. \quad (3)$$

For an eigenmode of the medium of Eq. (1), the determinant of the dyadic in Eq. (3) must be zero, given by [1]:

$$\det[\mu_0\omega^2\varepsilon_{ij} - q^2\delta_{ij} + q_iq_j] = 0. \quad (4)$$

Eq. (4) is the dispersion equation [2, 19] for the medium under consideration. The first solution of Eq. (4) corresponds to the ordinary mode with the electric field perpendicular to both the anisotropy axis and the wave vector:

$$q_x^2 + q_y^2 + q_z^2 = k^2. \quad (5)$$

The second solution corresponds to the extraordinary mode [2, 19]:

$$\varepsilon(q_y^2 + q_z^2) = \varepsilon\_(k^2 - q_x^2). \quad (6)$$

This is the object of our interest. One can see that extraordinary propagating modes exist in the negative uniaxial dielectric of Eq. (1) with $q_x \geq k$. Note that all eigenwaves of the negative uniaxial dielectric are the usual forward waves: wave vector **q** and Poynting vector **S** make an acute angle. It can be seen directly from Eq. (2) that

$$\mathbf{q} \cdot \mathbf{S} = \mathbf{q} \cdot (\mathbf{E} \times \mathbf{H})/2 = \mathbf{H} \cdot (\mathbf{q} \times \mathbf{E})/2 = \omega\mu_0H^2/2 > 0. \quad (7)$$

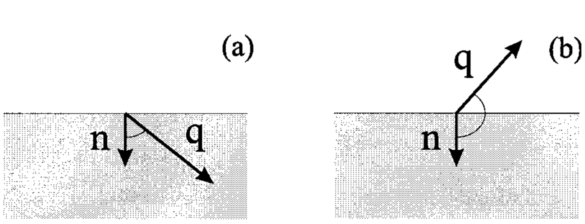

Figure 3 (a) Forward wave with respect to the interface $\mathbf{q} \cdot \mathbf{n} \geq 0$; (b) backward wave with respect to the interface $\mathbf{q} \cdot \mathbf{n} \leq 0$

4. BACKWARD WAVES WITH RESPECT TO INTERFACE WITHOUT NEGATIVE REFRACTION

Let us consider an interface (see Fig. 4) between an isotropic dielectric with permittivity $\tilde{\varepsilon}$ and a uniaxial dielectric with $\bar{\bar{\varepsilon}}$ described by Eq. (1). It is assumed that $\tilde{\varepsilon} > \varepsilon$. The interface is in the x–y plane and is illuminated by a TM plane wave coming from the isotropic dielectric. The wave vector $\mathbf{k}^i$ and electric field vector $\mathbf{E}^i$ lie in the x–z plane with $k_y^i = 0$, $E_y^i = 0$ (see Fig. 4).

In the case if $\varepsilon\_ > 0$, the total internal reflection corresponding to the inequality $\sin(\theta) > \sqrt{\varepsilon/\tilde{\varepsilon}}$ exists. But, if $\epsilon\_ < 0$, the situation is the opposite. For $\sin(\theta) < \sqrt{\varepsilon/\tilde{\varepsilon}}$, the wave will be completely reflected, but for the angles with $\sin(\theta) > \sqrt{\varepsilon/\tilde{\varepsilon}}$, some part of the wave will be transmitted through the interface.

Let us solve this reflection/transmission problem and show that in this case we have an example of backward wave with respect to interface and positive refraction. Using Eq. (6) we find the q_z component of the wave vector of the transmitted wave ($q_x = k_x = k^i\sin\,\theta$), given by

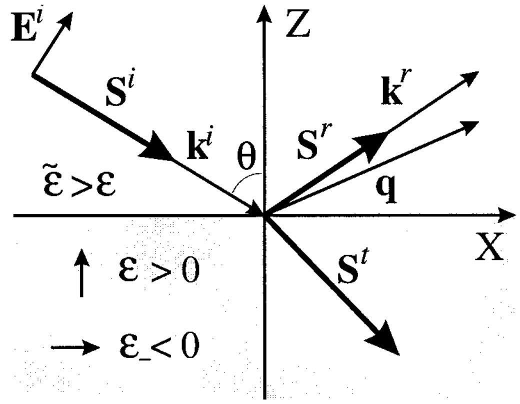

Figure 4 Backward wave with respect to interface without negative refraction

$$q_z = \pm k\sqrt{\frac{|\varepsilon\_|}{\varepsilon^2}(\tilde{\varepsilon}\sin^2\theta - \varepsilon)}. \quad (8)$$

The direction of the wave vector of the transmitted wave (the sign of q_z) cannot be determined at this stage. We need to choose correctly the direction of the power flow vector (Poynting vector) from the interface and only after that will we be able to determine the direction of the wave vector. Eq. (3) gives a relation for the components of the electric field $\mathbf{E}^t$ of the transmitted wave:

$$\varepsilon\_q_xE_x^t + \varepsilon q_zE_z^t = 0. \quad (9)$$

The boundary conditions give us the following relations among the amplitudes of the electric fields of the incident $\mathbf{E}^i$, reflected $\mathbf{E}^r$, and transmitted $\mathbf{E}^t$ waves:

$$\begin{cases} (E^i - E^r)\cos\,\theta = E_x^t \\ \tilde{\varepsilon}(E^i + E^r)\sin\,\theta = \varepsilon E_z^t \end{cases} \quad (10)$$

Together with Eq. (9), this forms a system of three equations with three unknowns, allowing us to calculate all the parameters of the problem. The calculation shows that in order to have the transmitted wave transmit energy from the interface into uniaxial medium, the following inequality must be satisfied:

$$\mathbf{z} \cdot \mathbf{S}^t = \frac{\omega\varepsilon\_}{2q_z}(E_x^t)^2 < 0. \quad (11)$$

Thus, one can see that $q_z > 0$, and we must choose the positive sign in relation (8). This means that the transmitted wave is a backward wave with respect to the interface.

On the other hand, we have

$$\mathbf{x} \cdot \mathbf{S}^t = \frac{\omega\varepsilon}{2q_x}(E_z^t)^2 > 0, \quad (12)$$

which means that we have positive refraction.

It is also interesting to study the expression for the reflection coefficient from the considered interface, given by

$$R = \frac{\varepsilon\_q_x \cos\theta - \tilde{\varepsilon} q_z \sin\theta}{\varepsilon\_q_x \cos\theta + \tilde{\varepsilon} q_z \sin\theta}. \tag{13}$$

We find that the reflection coefficient is equal to zero if

$$\sin\theta = \sqrt{\frac{\varepsilon(\tilde{\varepsilon} + |\varepsilon\_|)}{\tilde{\varepsilon}^2 + \varepsilon|\varepsilon\_|}}. \tag{14}$$

Such a real angle always exists and is found in the region $1 > \sin(\theta) > \sqrt{\varepsilon/\tilde{\varepsilon}}$ if $\tilde{\varepsilon} > \varepsilon$. The wave incident with such an angle completely transmits with positive refraction into the uniaxial dielectric and becomes backward with respect to interface.

If one would like to have identical described effects in any plane of incidence (not only OXZ, as was considered) the following double negative uniaxial dielectric should be used instead of Eq. (1):

$$\bar{\bar{\varepsilon}} = \varepsilon\_(\mathbf{xx} + \mathbf{yy}) + \varepsilon\mathbf{zz}, \tag{15}$$

with $\varepsilon\_ < 0$, $\varepsilon > 0$.

5. NEGATIVE REFRACTION WITHOUT BACKWARD WAVES WITH RESPECT TO INTERFACE

Next, consider an interface in the y–z plane (see Fig. 5) illuminated by a TM plane wave coming from the isotropic dielectric with the wave vector $\mathbf{k}^i$ and electric field vector $\mathbf{E}^i$ lying in the x–z plane with $k^i_y = 0$, $E^i_y = 0$ (see Fig. 5). In this case the refracted wave exists for all possible incidence angles and it will be shown that we have examples of negative refraction, but forward wave with respect to interface.

Using Eq. (6) we find the q_x component of the wave vector of transmitted wave ($q_z = k_z = k^i \sin\theta$), given by

$$q_x = \pm k\sqrt{1 - \frac{\tilde{\varepsilon}}{\varepsilon\_}\sin^2\theta}. \tag{16}$$

As in the previous case we will choose the sign of q_x on the base of the correct direction of the power flow vector (Poynting vector) from the interface. Relation (9) is still valid, but the system of Eq. (10) transforms to

$$\begin{cases} (E^i - E^r)\cos\theta = E^t_x \\ \tilde{\varepsilon}(E^i + E^r)\sin\theta = \varepsilon\_E^t_z. \end{cases} \tag{17}$$

The inequality in Eq. (11), corresponding to the demand for the transmitted wave to transfer energy from the interface into the uniaxial medium, transforms to

$$\mathbf{x}\cdot\mathbf{S}^t = \frac{\omega\varepsilon}{2q_x}(E^t_z)^2 < 0, \tag{18}$$

and it follows that we must take the negative sign in Eq. (16). Thus, we have a forward wave with respect to interface.

On the other hand, we have

$$\mathbf{z}\cdot\mathbf{S}^t = \frac{\omega\varepsilon\_}{2q_z}(E^t_x)^2 < 0, \tag{19}$$

which means that we have a negative refraction phenomenon.

The reflection coefficient from considered interface is

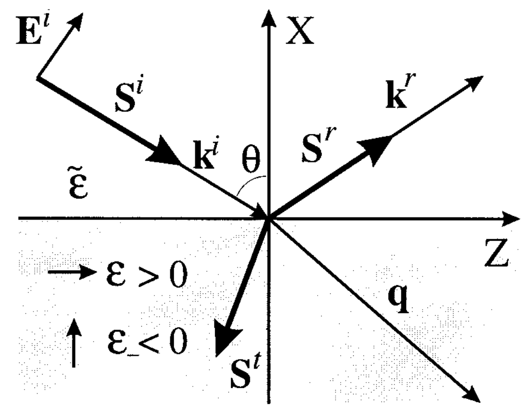

Figure 5 Negative refraction with forward wave with respect to the interface

$$R = \frac{\varepsilon^2_- q_x \cos\theta - \tilde{\varepsilon}\varepsilon q_z \sin\theta}{\varepsilon^2_- q_x \cos\theta + \tilde{\varepsilon}\varepsilon q_z \sin\theta}. \tag{20}$$

One can see that reflection coefficient is equal to zero if

$$\sin\theta = \sqrt{\frac{|\varepsilon\_|^3 + \tilde{\varepsilon}\varepsilon^2}{|\varepsilon\_|^3 + \tilde{\varepsilon}^2\varepsilon}}. \tag{21}$$

In the same manner as in the previous case, such a real angle exists if $\varepsilon < \tilde{\varepsilon}$ and is found in region $1 > \sin(\theta) > \sqrt{\varepsilon/\tilde{\varepsilon}}$. The wave incident with such an angle completely transmits into the uniaxial dielectric with negative refraction and remains a forward wave with respect to interface.

Note that the described effect of negative refraction can be observed for any plane of incidence (not only OXZ, as was considered).

6. CONCLUSION

In this paper we have presented simple examples of possibilities of negative refraction without backward waves, and backward waves with respect to the interface without negative refraction, for homogeneous TM plane waves. The examples are based on uniaxial dielectric with negative permittivity along the anisotropy axis. The material is completely nonmagnetic.

ACKNOWLEDGMENTS

The author would like to acknowledge C. R. Simovski, S. A. Tretyakov, I. S. Nefedov, and S. I. Maslovski for helpful and useful discussions. He thanks the SUMMA Foundation for their support under a SUMMA Graduate Fellowship in Advanced Electromagnetics.

REFERENCES

1. V. Veselago, Sov Phys Usp 10 (1968), 509.
2. I. Lindell, S. Tretyakov, K. Nikoskinen, and S. Ilvonen, Microwave Optical Technol Lett 31 (2001), 129.
3. R. Ruppin, J Phys Condens Matter 13 (2001), 1811.
4. D.R. Smith and N. Knoll, Phys Rev Lett 85 (2000), 2933.
5. R. Shelby, D. Smith, and S. Schultz, Sci 292 (2001), 77.
6. D. Smith, W. Padilla, D. Vier, S. Nemat-Nasser, and S. Schultz, Phys Rev Lett 84 (2000), 4184.
7. C. Caloz, C.-C. Chang, and T. Itoh, J Appl Phys 90 (2001), 5483.
8. R.W. Ziolkowski and E. Heyman, Phys Rev E 64 (2001), 056625.
9. J. Pendry, Phys Rev Lett 85 (2000), 3966.
10. N. Engheta, Ant Wireless Propag Lett 1 (2002), 10.

11. R. Silin and I. Chepurnih, J Commun Technol Electr 46 (2001), 1121.
12. M. Notomi, Phys Rev B 62 (2000), 10696.
13. M. Notomi, Opt Quantum Electr 34 (2002), 133.
14. C. Luo, S. Johnson, J. Jannopopoulous, and J. Pendry, Phys Rev B 65 (2002), 201104.
15. C. Luo, S. Johnson, and J. Jannopopoulous, Appl Phys Lett 81 (2002), 2352.
16. J. Shen and P. Platzman, Appl Phys Lett 80 (2002), 3286.
17. J. Pendry and S. Ramakrishna, J Phys: Condens Matter 14 (2002), 8463.
18. S. Ramakrishna, J. Pendry, D. Schurig, D. Smith, and S. Schultz, J Modern Optics 49 (2002), 1747.
19. V. Ginzburg, The propagation of electromagnetic waves in plasmas, Pergamon, Oxford, 1964.

A HIGHLY EFFICIENT AND ACCURATE PROCEDURE FOR SEMI-ANECHOIC CHAMBER ANALYSIS USING CIRCUITAL TECHNIQUES

L. Nuño, J. V. Balbastre, and F. D. Quesada
Asociación ITACA
Universidad Politécnica de Valencia
Camino de Vera s/n
46022, Valencia, Spain

Received 8 November 2002

ABSTRACT: *This paper reports on a new method for the determination of the performance qualities of a semi-anechoic chamber used for electromagnetic compatibility measurements. This approach, based on highly efficient and accurate circuital techniques, provides very good results on low-cost desktop computers in the frequency range 30–300 MHz.* © 2003 Wiley Periodicals, Inc. Microwave Opt Technol Lett 37: 263–265, 2003; Published online in Wiley InterScience (www.interscience.wiley.com). DOI 10.1002/mop.10888

Key words: *anechoic chamber; geometrical optics; electromagnetic compatibility*

INTRODUCTION

The design of semi-anechoic chambers for electromagnetic compatibility (EMC) measurements is a very complex process and manufacturers usually carry out their designs on an eminently empirical basis. Currently, different methods to evaluate the expected operation of anechoic and semi-anechoic chambers are used. The most typical one, due to its simplicity, is the ray tracing technique [1]. This approach assumes that both the transmitting and the receiving antennae are sited in the far-field area and that the waves are locally planed on the chamber walls. The method uses geometrical optics (GO) to calculate the waves reflected by the walls and considers one or more reflections depending on the desired accuracy. All these assumptions cause the ray tracing technique to be inaccurate at frequencies lower than 100 MHz. In order to study the chamber behavior below this limit, methods based on the direct resolution of Maxwell's equations must be used, such as the finite-element method (FEM) [2], the finite-integration technique (FIT) [3], or the finite-difference time-domain (FDTD) method [4]. All these approaches transform the 3D Maxwell's equations into an algebraic problem and provide the full-wave electromagnetic field in a finite set of points. However, the accuracy of these methods strongly depends on the size of the final algebraic problem and, for actual chamber analysis, they become rather slow and require huge amounts of computer memory. To achieve good results in a reasonable time it is necessary to use very expensive and large multiprocessor computers. There are various technological alternatives to cover the walls of the chamber in order to reduce the reflected power and make it operate like an open area test site (OATS) [5]. The work presented in this paper focuses on the analysis of those chambers using ceramic ferrite tiles. To this end, a new and very accurate method with a relatively low computational cost has been developed for the analysis of semi-anechoic chambers in the range of frequencies between 30 MHz and 300 MHz. This method has been validated by comparing the computed results with measurements performed inside a real chamber.

THEORETICAL DEVELOPMENT

Our developed method is based on the application of modal analysis on Cartesian coordinates, combined with techniques similar to those used in microwave circuit theory [6]. The analysis of the chamber is performed for two orthogonal polarizations—horizontal and vertical—defined according to the chamber floor, which is considered as an electric wall. For the sake of symmetry, only half of the structure is analyzed. To this end, an electric or magnetic wall is situated on the horizontal plane (for cases of vertical and horizontal polarization, respectively), as shown in Figure 1. The walls, covered with absorbent material, are treated as if they were ports in a microwave network and numbered 1 to 4 (see Fig. 1).

The solution for the Maxwell's equations in the empty volume of the semi-anechoic chamber is decomposed as an addition of the homogeneous solution plus a particular solution of the inhomogeneous equation. The homogeneous solution may be obtained by using the modal analysis method as a summation of rectangular harmonics. The effect of the walls on the homogeneous component of the field is taken into account by means of the [F] matrix, which relates certain tangential components of the homogeneous electric and magnetic fields at each port, given by

$$[H^h] = [F][E^h], \tag{1}$$

where $[E^h]$ and $[H^h]$ are the vectors of the modal coefficients from the homogeneous electric and magnetic fields, respectively.

The effect of the absorbent walls on the total field is considered by means of a generalized admittance matrix $[Y]$, which relates certain components of the total tangential electric and magnetic fields at each port, given by

$$[H] = [Y][E] \tag{2}$$

with $[H]$ and $[E]$ the modal coefficient vectors from the total electric and magnetic fields within the chamber, respectively. If the walls are covered with ferrite tiles over a dielectric layer (usually wood), the admittance matrix may be obtained, assuming that the ports are uncoupled with each other (the admittance matrix will then be block diagonal). To calculate the admittance sub-matrices corresponding to each access we have used a model of shorted waveguides, through which the corresponding modes propagate. The total electric and magnetic fields may be decomposed, as mentioned above, as the addition of the homogeneous and the inhomogeneous field vectors:

$$[H] = [H^h] + [H^i], \quad [E] = [E^h] + [H^i], \tag{3}$$